Electronic Theory for Cleaved Alloys: Effects of Off-Diagonal Disorder

Kin-ichi Masuda

Department of Materials Science and Engineering, Tokyo Institute of Technology, Ookayama, Meguro, Tokyo 152, Japan

Z. Naturforsch. **33 a**, 1212–1223 (1978); received July 18, 1978

The tight-binding type theory for cleaved alloys by Bennemann et al. has been extended to include the effects of the random transfer integrals (off-diagonal disorder). The chemisorption and segregation behavior of cleaved alloys is investigated in detail including both the diagonal and off-diagonal disorder. It is demonstrated that the effects of the off-diagonal disorder are very important for the electronic properties of cleaved alloys. The theory has further been used to study the electronic structure of metal surfaces with substitutional disorder as well as to investigate the changes in the density of states due to the order-disorder phase transition in chemisorbed layers.

1. Introduction

An understanding of the surface of transition metal alloys is of great importance in relation to catalysis by alloys, corrosion and segregation phenomena. Indeed it is known that some transition metal alloys (e.g. CuNi) exhibit catalytic behavior with interesting technical applications [1, 2]. Atomic segregation phenomena at the surface have been observed on many transition metal alloys such as PdAg, PdAu, NiCu, NiAu, PtAg [3–8], and ZrFe [9] alloys. In order to understand these interesting experimental findings from a theoretical point of view, it is desirable to develop a microscopic electronic theory for treating d-electrons near the surface.

So far, however, only a few theories * have been presented for treating d-electrons at the surface of transition metal alloys, and the above mentioned surface phenomena have not been fully discussed. Bennemann and his co-workers [11–13] have developed a tight-binding type theory for d-electrons at the surface of transition metal alloys. The electron scattering due to the atomic disorder (only the diagonal disorder) is treated by using the continued fraction method. Desjonquères and Cyrot-Lackmann [14] have presented the more elaborate moment theory for the electronic structure of cleaved alloys: The electronic density of states of bulk and cleaved binary alloys is determined through a tight-binding model, using a continued fraction technique and a computer simulation on clusters of several thousands of atoms. In general, one can obtain with these two methods essentially the same results for the electronic structure [12]. In this respect, the former theory does have the virtue of being simple for numerical calculations.

It is the purpose of the present paper to extend the tight-binding type theory for cleaved alloys by Bennemann et al. to include the effects of the random transfer integrals (off-diagonal disorder) between nearest neighbours. It is quite desirable to include the off-diagonal disorder in an alloy theory so as to permit a study of alloys of materials having different bandwidth. It is to be noted that the pure components of real alloys have always different band structures and random off-diagonal elements occure in the alloy Hamiltonian. The formal theory for cleaved alloys with both diagonal and off-diagonal disorder is presented in Sect. 2 and numerical results on electronic structures are given in Section 3. The chemisorption and segregation behavior of cleaved alloys is investigated in Sect. 4 and Sect. 5, respectively, including both diagonal and off-diagonal disorder.

Furthermore, we present some of the applications of the present theory: In Appendix A, we study the electronic structure of cleaved metals with substitutional disorder (both diagonal and off-diagonal disorder) in the surface layer (referred to as system A). This calculation is useful when studying the surface segregation of dilute alloys [15–16]. In Appendix B, we further investigate the changes in the electronic density of states due to the order disorder phase transition in chemisorbed layers (system B). These studies have been motivated by

* The first electronic theory for cleaved alloys is Berk's CPA theory [10]. However, the continued fraction technique mentioned below is more appropriate to treat cleaved alloys.

the following considerations: The Green's function theory of the Kalkstein-Soven type [17—20] is probably incapable of treating system A when the off-diagonal disorder is introduced in the surface layer and is only applicable to system B when the order parameter η is one (complete order case) or zero (complete disorder case).

2. Tight-Binding Theory for Cleaved Alloys

We describe the d-electrons in a transition metal alloy by the usual tight-binding Hamiltonian and use the well known s-band approximation with five independent s-orbitals per atom:

$$H = \sum_i E_i c_i^\dagger c_i + \sum_{i \neq j} T_{ij} c_i^\dagger c_j , \tag{1}$$

where $c_i^\dagger (c_j)$ is the creation (annihilation) operator for the d-electron on site $i\,(j)$. The hopping integrals T_{ij} describe the electronic transitions between atomic sites i and j and the electronic energy level E_i takes the values E_A and E_B depending on whether the site i is occupied by an A-atom or a B-atom. The local electronic Green's function $G_{ii}(E)$ for electrons on site i is given by

$$G_{ii}(E) = (E - E_i - \Delta_i)^{-1} , \tag{2}$$

where the electron self-energy Δ_i results from all hopping processes starting and ending on site i and is expressed as

$$\Delta_i = \sum_{j \neq i} \frac{T_{ij} T_{ji}}{E - E_j - \Delta_j^i} + \sum_{\substack{j \neq i \\ l \neq i,j}} \frac{T_{ij} T_{jl} T_{li}}{(E - E_j - \Delta_j^i)(E - E_l - \Delta_l^{ij})} + \cdots , \tag{3a}$$

with

$$\Delta_j^i = \sum_{l \neq i,j} \frac{T_{jl} T_{lj}}{E - E_l - \Delta_l^{ij}} + \cdots . \tag{3b}$$

Here, the self-energy $\Delta_j^i\,(\Delta_l^{ij})$ results from hopping processes starting and ending at the site $j\,(l)$ and avoiding the site i (sites i and j) in between.

In order to close the expansion (3a), we keep only the terms of the order T^2 and use the approximation $\Delta_l^{ij} = \Delta_l^j$ [12], which is exact for a Bethe lattice [21]. Here, it is important to realize that (i) the approximation on Δ_l^{ij} should become better at the surface since the number of neglected paths is smaller, (ii) the terms of higher than T^2 in Eq. (3a) essentially affect only the fine structure of the electronic density of states and of little importance for the semi-quantitative understanding of the alloy surfaces [12]. In the calculation of the electronic Green's function we assume that the surface affects only the d-electrons within the first three atomic layers at the surface. This assumption seems to be quite reasonable in view of the exact Green's function calculations on the electronic structures of cleaved metals of [17].

We now apply the above theory to d-electrons at the surface of (transition metal) alloys with both the diagonal and off-diagonal disorders. The average d-electron Green's function in the L-th atomic layer is

$$G_L(E) = C_A G_{LA}(E) + (1 - C_A) G_{LB}(E) , \tag{4}$$

where $L = \mathrm{I}, \mathrm{II}, \mathrm{III} \ldots$, and the local Green's functions are given by

$$G_{Li}(E) = (E - E_{Li} - \Delta_{Li})^{-1} . \tag{5}$$

Here E_{Li} and Δ_{Li} denote the site energy and the self-energy for atomic sites i (A or B) in the L-th layer. From Eqs. (3a) and (3b), one finds that

$$\Delta_{\mathrm{IA}} = \frac{Z_0 C_A T_{AA}^2}{E - E_{\mathrm{IA}} - \Delta_{\mathrm{IA}}^{\mathrm{I}}} + \frac{Z_0 C_B T_{AB}^2}{E - E_{\mathrm{IB}} - \Delta_{\mathrm{IB}}^{\mathrm{I}}} + \frac{Z_1 C_A T_{AA}^2}{E - E_{\mathrm{IIA}} - \Delta_{\mathrm{IIA}}^{\mathrm{I}}} + \frac{Z_1 C_B T_{AB}^2}{E - E_{\mathrm{IIB}} - \Delta_{\mathrm{IIB}}^{\mathrm{I}}} , \tag{6}$$

$$\Delta_{\mathrm{IB}} = \frac{Z_0 C_A T_{BA}^2}{E - E_{\mathrm{IA}} - \Delta_{\mathrm{IA}}^{\mathrm{I}}} + \frac{Z_0 C_B T_{BB}^2}{E - E_{\mathrm{IB}} - \Delta_{\mathrm{IB}}^{\mathrm{I}}} + \frac{Z_1 C_A T_{BA}^2}{E - E_{\mathrm{IIA}} - \Delta_{\mathrm{IIA}}^{\mathrm{I}}} + \frac{Z_1 C_B T_{BB}^2}{E - E_{\mathrm{IIB}} - \Delta_{\mathrm{IIB}}^{\mathrm{I}}} , \tag{7}$$

$$\Delta_{\mathrm{IIA}} = \frac{Z_0 C_A T_{AA}^2}{E - E_{\mathrm{IIA}} - \Delta_{\mathrm{IIA}}^{\mathrm{II}}} + \frac{Z_0 C_B T_{AB}^2}{E - E_{\mathrm{IIB}} - \Delta_{\mathrm{IIB}}^{\mathrm{II}}} + \frac{Z_1 C_A T_{AA}^2}{E - E_{\mathrm{IIIA}} - \Delta_{\mathrm{IIIA}}^{\mathrm{II}}} + \frac{Z_1 C_B T_{AB}^2}{E - E_{\mathrm{IIIB}} - \Delta_{\mathrm{IIIB}}^{\mathrm{II}}} + \frac{Z_1 C_A T_{AA}^2}{E - E_{\mathrm{IA}} - \Delta_{\mathrm{IA}}^{\mathrm{II}}} + \frac{Z_1 C_B T_{AB}^2}{E - E_{\mathrm{IB}} - \Delta_{\mathrm{IB}}^{\mathrm{II}}} , \tag{8}$$

$$\Delta_{\mathrm{IIB}} = \frac{Z_0 C_A T_{BA}^2}{E - E_{\mathrm{IIA}} - \Delta_{\mathrm{IIA}}^{\mathrm{II}}} + \frac{Z_0 C_B T_{BB}^2}{E - E_{\mathrm{IIB}} - \Delta_{\mathrm{IIB}}^{\mathrm{II}}} + \frac{Z_1 C_A T_{BA}^2}{E - E_{\mathrm{IIIA}} - \Delta_{\mathrm{IIIA}}^{\mathrm{II}}} + \frac{Z_1 C_B T_{BB}^2}{E - E_{\mathrm{IIIB}} - \Delta_{\mathrm{IIIB}}^{\mathrm{II}}} + \frac{Z_1 C_A T_{BA}^2}{E - E_{\mathrm{IA}} - \Delta_{\mathrm{IA}}^{\mathrm{II}}} + \frac{Z_1 C_B T_{BB}^2}{E - E_{\mathrm{IB}} - \Delta_{\mathrm{IB}}^{\mathrm{II}}} . \tag{9}$$

In the above equations, we denote the number of nearest neighbour atoms within the same layer by Z_0 and the number of nearest neighbour atoms within one of the adjacent layers by Z_1. The self-energies for the third layer, Δ_{IIIA} and Δ_{IIIB}, are given by the similar expressions to Δ_{IIA} and Δ_{IIB}. The self-energies of the types $\Delta^{\mathrm{I}}_{\mathrm{IA}}$, $\Delta^{\mathrm{I}}_{\mathrm{IB}}$, $\Delta^{\mathrm{I}}_{\mathrm{IIA}}$, ..., are obtained by using the approximation $\Delta_l{}^{ij} = \Delta_l{}^{j}$. For example, for $\Delta^{\mathrm{I}}_{\mathrm{IA}}$ and $\Delta^{\mathrm{I}}_{\mathrm{IIA}}$ one finds that

$$\Delta^{\mathrm{I}}_{\mathrm{IA}} = \frac{(Z_0-1)\,C_{\mathrm{A}}\,T^2_{\mathrm{AA}}}{E-E_{\mathrm{IA}}-\Delta^{\mathrm{I}}_{\mathrm{IA}}} + \frac{(Z_0-1)\,C_{\mathrm{B}}\,T^2_{\mathrm{AB}}}{E-E_{\mathrm{IB}}-\Delta^{\mathrm{I}}_{\mathrm{IB}}} + \frac{Z_1\,C_{\mathrm{A}}\,T^2_{\mathrm{AA}}}{E-E_{\mathrm{IIA}}-\Delta^{\mathrm{I}}_{\mathrm{IIA}}} + \frac{Z_1\,C_{\mathrm{B}}\,T^2_{\mathrm{AB}}}{E-E_{\mathrm{IIB}}-\Delta^{\mathrm{I}}_{\mathrm{IIB}}}, \tag{10}$$

$$\Delta^{\mathrm{I}}_{\mathrm{IIA}} = \frac{Z_0\,C_{\mathrm{A}}\,T^2_{\mathrm{AA}}}{E-E_{\mathrm{IIA}}-\Delta^{\mathrm{II}}_{\mathrm{IIA}}} + \frac{Z_0\,C_{\mathrm{B}}\,T^2_{\mathrm{AB}}}{E-E_{\mathrm{IIB}}-\Delta^{\mathrm{II}}_{\mathrm{IIB}}} + \frac{Z_1\,C_{\mathrm{A}}\,T^2_{\mathrm{AA}}}{E-E_{\mathrm{IIIA}}-\Delta^{\mathrm{II}}_{\mathrm{IIIA}}} + \frac{Z_1\,C_{\mathrm{B}}\,T^2_{\mathrm{AB}}}{E-E_{\mathrm{IIIB}}-\Delta^{\mathrm{II}}_{\mathrm{IIIB}}} + \frac{(Z_1-1)\,C_{\mathrm{A}}\,T^2_{\mathrm{AA}}}{E-E_{\mathrm{IA}}-\Delta^{\mathrm{II}}_{\mathrm{IA}}} + \frac{(Z_1-1)\,C_{\mathrm{B}}\,T^2_{\mathrm{AB}}}{E-E_{\mathrm{IB}}-\Delta^{\mathrm{II}}_{\mathrm{IB}}}. \tag{11}$$

Then we get from Eq. (3b) a set of eighteen coupled equations with $\Delta^{\mathrm{I}}_{\mathrm{IA}}$, $\Delta^{\mathrm{I}}_{\mathrm{IB}}$, $\Delta^{\mathrm{II}}_{\mathrm{IA}}$, $\Delta^{\mathrm{II}}_{\mathrm{IB}}$, $\Delta^{\mathrm{I}}_{\mathrm{IIA}}$, $\Delta^{\mathrm{I}}_{\mathrm{IIB}}$, $\Delta^{\mathrm{II}}_{\mathrm{IIA}}$, $\Delta^{\mathrm{II}}_{\mathrm{IIB}}$, $\Delta^{\mathrm{III}}_{\mathrm{IIA}}$, $\Delta^{\mathrm{III}}_{\mathrm{IIB}}$, $\Delta^{\mathrm{II}}_{\mathrm{IIIA}}$, $\Delta^{\mathrm{II}}_{\mathrm{IIIB}}$, $\Delta^{\mathrm{III}}_{\mathrm{IIIA}}$, $\Delta^{\mathrm{III}}_{\mathrm{IIIB}}$, $\Delta^{b}_{\mathrm{IIIA}}$, $\Delta^{\mathrm{III}}_{b\mathrm{A}}$, and $\Delta^{\mathrm{III}}_{b\mathrm{B}}$ as unknowns in terms of T_{AA}, T_{AB}, T_{BB}, Z_0, Z_1, $E_{\mathrm{I}i}$, $E_{\mathrm{II}i}$, $E_{\mathrm{III}i}$, E_{bi}, and Δ^{b}_{bi} (b refers to the bulk or forth layer). For the case where the off-diagonal disorders can be neglected, the electronic Green's functions $G_{\mathrm{I}i}(E)$, $G_{\mathrm{II}i}(E)$ and $G_{\mathrm{III}i}(E)$ are determined from the six coupled equations for the self-energies as shown in [12].

The self-energies for the bulk layer are given from Eq. (3a) as

$$\Delta_{b\mathrm{A}} = \frac{(Z_0+2Z_1)\,C_{\mathrm{A}}\,T^2_{\mathrm{AA}}}{E-E_{b\mathrm{A}}-\Delta^{b}_{b\mathrm{A}}} + \frac{(Z_0+2Z_1)\,C_{\mathrm{B}}\,T^2_{\mathrm{AB}}}{E-E_{b\mathrm{B}}-\Delta^{b}_{b\mathrm{B}}}, \tag{12}$$

$$\Delta_{b\mathrm{B}} = \frac{(Z_0+2Z_1)\,C_{\mathrm{A}}\,T^2_{\mathrm{BA}}}{E-E_{b\mathrm{A}}-\Delta^{b}_{b\mathrm{A}}} + \frac{(Z_0+2Z_1)\,C_{\mathrm{B}}\,T^2_{\mathrm{BB}}}{E-E_{b\mathrm{B}}-\Delta^{b}_{b\mathrm{B}}}, \tag{13}$$

where

$$\Delta^{b}_{b\mathrm{A}} = (Z_0+2Z_1-1)\cdot\left\{\frac{C_{\mathrm{A}}\,T^2_{\mathrm{AA}}}{E-E_{b\mathrm{A}}-\Delta^{b}_{b\mathrm{A}}} + \frac{C_{\mathrm{B}}\,T^2_{\mathrm{AB}}}{E-E_{b\mathrm{B}}-\Delta^{b}_{b\mathrm{B}}}\right\}, \tag{14}$$

$$\Delta^{b}_{b\mathrm{B}} = (Z_0+2Z_1-1)\cdot\left\{\frac{C_{\mathrm{A}}\,T^2_{\mathrm{BA}}}{E-E_{b\mathrm{A}}-\Delta^{b}_{b\mathrm{A}}} + \frac{C_{\mathrm{B}}\,T^2_{\mathrm{BB}}}{E-E_{b\mathrm{B}}-\Delta^{b}_{b\mathrm{B}}}\right\}. \tag{15}$$

The Eqs. (14) and (15) can be rewritten as a fourth-order equation in $\Delta^{b}_{b\mathrm{A}}$ or $\Delta^{b}_{b\mathrm{B}}$ as a function of Z_0, Z_1, $E_{b\mathrm{A}}$, $E_{b\mathrm{B}}$, C_{A}, T_{AA}, T_{AB} and T_{BB}. In particular, if the transfer integrals T_{AA}, T_{AB} and T_{BB} satisfy Shiba's condition [22], i.e.

$$T_{\mathrm{AB}} = (T_{\mathrm{AA}}\cdot T_{\mathrm{BB}})^{1/2},$$

the fourth-order equation reduce to the cubic equation:

$$\begin{aligned}\alpha^{-2}(\Delta^{b}_{b\mathrm{A}})^3 &- \{E-E_{b\mathrm{B}}+\alpha^{-2}(E-E_{b\mathrm{A}})\}(\Delta^{b}_{b\mathrm{A}})^2 \\ &+ \{(E-E_{b\mathrm{A}})(E-E_{b\mathrm{B}}) \\ &+ (Z_0+2Z_1-1)\,T^2\}\,\Delta^{b}_{b\mathrm{A}} \\ &- (Z_0+2Z_1-1)\,T^2\{\alpha^2\,C_{\mathrm{A}}(E-E_{b\mathrm{B}}) \\ &+ C_{\mathrm{B}}(E-E_{b\mathrm{A}})\} = 0,\end{aligned} \tag{16}$$

where $T_{\mathrm{AA}}=\alpha T$, $T_{\mathrm{BB}}=\alpha^{-1}T$ and $T_{\mathrm{AB}}=T$. If $\alpha=1$ (diagonal disorder problem), eq. (16) further reduces to that obtained by Morán-López, Kerker and Bennemann [12]. The expression for Δ^{b}_{bi} given by Eq. (14) or (15) is equivalent to the one used in the coherent locator formalism for disordered bulk alloys by Shiba [22].

Once the self-energies for the bulk layer are obtained, the eighteen coupled equations for the self-energies (Eqs. (10), (11), etc.) are solved quite easily by the iterative procedure. (At the first stage of the iteration, the self-energies $\Delta_i{}^{j}$ for the cleaved alloy are replaced by those for the bulk alloy.) The electronic density of states for an atom of type i within the L-th layer is determined from the electronic Green's function by the formula

$$\varrho_{Li}(E) = -(1/\pi)\cdot \mathrm{Im}\,G_{Li}(E). \tag{17}$$

3. Numerical Results for the Electronic Density of States of Cleaved Alloys

In this section we present the electronic density of states for the cleaved alloys with both the diagonal and off-diagonal disorders. In particular, we have considered the following two cases in our numerical examples; (a) (100) cleaved simple cubic (sc) lattice, and (b) (100) cleaved face centered cubic (fcc) lattice, with parameter values appropriate for CuNi or AgPd alloys. Though the present method is capable of treating the general off-diagonal disorder, we restrict ourselves in the present numerical calculations to two types of the off-diagonal disorders; one is the Shiba-type off-diagonal disorder and the other is the additive-type off-diagonal disorder ($T_{\mathrm{AB}}=(T_{\mathrm{AA}}+T_{\mathrm{BB}})/2$).

3.1. (100) Cleaved Simple Cubic Lattice

Assuming the additive-type off-diagonal disorder, we have numerically evaluated the electronic density of states for the simple cubic alloy with (100) surface. In this case, $Z_0 = 4$ and $Z_1 = 1$, and the eighteen coupled equations for the self-energies (Eqs. (10), (11), etc.) are solved by the iterative procedure. After 20 or 30 iterations, the self-energies of the type Δ_j^i converge to the final values. In Fig. 1 we present the average electronic density of states for the (100) surface (full curve) of the sc alloy with parameters: $C_A = 0.6$ and 0.9, $\delta_L (= E_{LA} - E_{LB}) = 0.4$ and 1.5, and $T_{AA}(T_{BB}) =$ 1.5(0.5), 1.2(0.8), 0.8(1.2), 0.5(1.5). Also shown (dashed curve) is the corresponding density of states for the bulk layer. The parameter values are chosen so as to facilitate the comparison of the present results for the bulk layer with those obtained by Blackmann et al. (generalized-locator renormalized-interactor formalism) [23]. The unit of the energy is taken to be the half-bandwidth of the unperturbed crystal ($E_{LA} = E_{LB}$ and $T_{AA} = T_{BB} = T_{AB}$), which is set equal to 1. The zero of energy is chosen in such a way that $E_{LA} = -E_{LB} = \delta_L/2$.

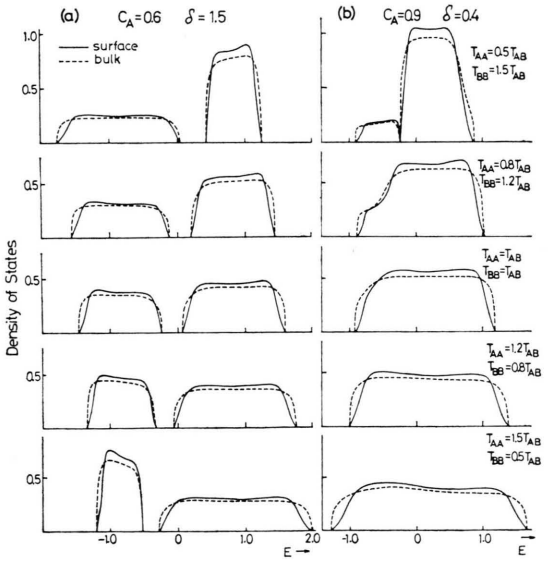

Fig. 1. Average density of states $\varrho_L(E)$ of the surface (solid curve) and bulk (dashed curve) layers for the (100) cleaved sc alloys. (a) $C_A = 0.6$ and $\delta = 1.5$, (b) $C_A = 0.9$ and $\delta = 0.4$. The energy is in units of the half-bandwidth of the unperturbed crystal ($E_{LA} = E_{LB}$ and $T_{AA} = T_{BB} = T_{AB}$).

The bottom curve of the set in Fig. 1 ((a) and (b)) illustrates the average electronic density of states of an alloy for which the pure host (A) band is three times wider than, and overlaps, the pure solute (B) band. As we move up through the set of curves, the host band narrows while the solute band broadens. In each case, the host (A) band is centered above the solute band center. The strong effects of the different constituent bandwidths are clearly seen in the figures, both for the surface and for the bulk layers. Comapring the results in Fig. 1 with those in Ref. [23], one can see that the general behavior of the $\varrho_{\text{bulk}}(E)$ are quite similar to those obtained by Blackmann et al. [23]. This indicates that the present tight-binding theory should give correctly the overall shape of the electronic density of states for the bulk as well as for the surface layers.

3.2. (100) Cleaved FCC Lattice

For the (100) fcc alloy, $Z_0 = Z_1 = 4$, and the eighteen coupled equations for the self-energies of the type Δ_j^i are solved by iteration, again. The electronic density of states $\varrho_{Li}(E)$ is calculated using the formula of Eq. (17). In Figs. 2 and 3 we present the average as well as the local electronic densities of states in the first three layers of the (100) cleaved fcc alloys, together with those for the bulk

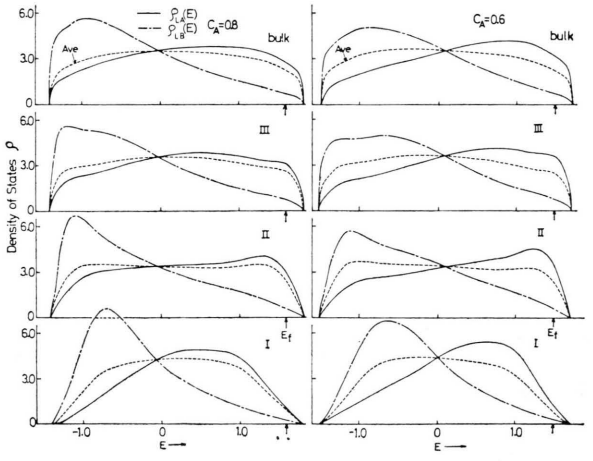

Fig. 2. Local density of states $\varrho_{Li}(E)$ of the first three surface layers (L = I, II, III) and a bulk layer of the (100) cleaved fcc alloy (which roughly represents the CuNi alloys). $E_A (= E_{Ni}) = -E_B (= E_{Cu}) = \delta/2$. $\delta = 0.6$, $T_{AA} = 1.2\,T_{BB}$ and (a) $C_A = 0.8$, (b) $C_A = 0.6$. The energy is in units of the half of the B(Cu)-metal d-bandwidth ($\sim$ 1.7 eV). Also shown (dashed curve) is the average density of states.

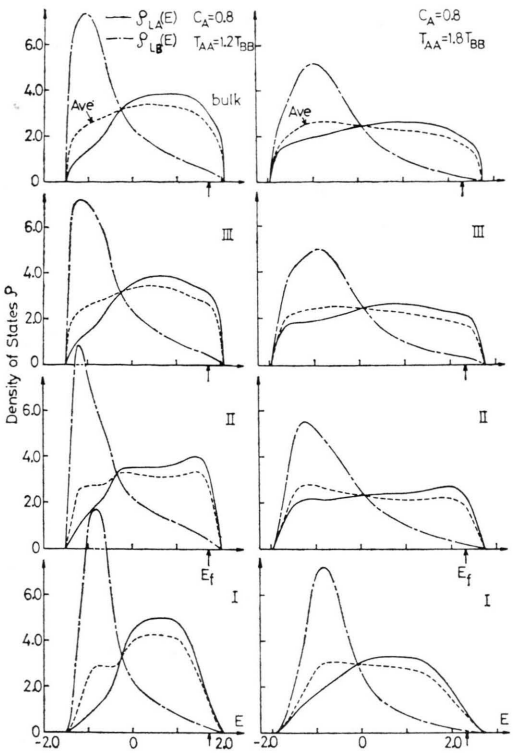

Fig. 3. Local density of states $\varrho_{Li}(E)$ of the first three surface layers and a bulk layer of the (100) cleaved alloy (the curves in (b) roughly represent the AgPd alloys). $E_A(=E_{Pd})=-E_B(=E_{Ag})=\delta/2$, $\delta=1.0$, $T_{AA}=1.2\,T_{BB}$ and $1.8\,T_{BB}$, $T_{AB}=(T_{AA}\cdot T_{BB})^{1/2}$.

layer. The parameter values of δ_L and the transfer integrals ($T_{AB}=(T_{AA}\cdot T_{BB})^{1/2}$) are chosen to describe the CuNi [24] or AgPd [25] alloys: $\delta_L(=E_{LA}-E_{LB})=0.6$ and 1.0 for $L=$ I, II, III, and b (in units of the half of the Cu (or Ag) d-bandwidth, ~ 1.7 eV) and $T_{AA}=1.2\,T_{BB}$ and $1.8\,T_{BB}$ (B refers to the noble metal atom Cu or Ag). Note, the d-bandwidth of Ni(Pd) is about 20(80)% wider than that of Cu(Ag).

In the present calculation, we neglect electronic charge transfer between the Cu(Ag) and Ni(Pd) atoms as in Refs. [12] and [24], since the Fermi energy of Cu(Ag) and Ni(Pd) are almost the same. This is also confirmed by the fact that by neglecting electronic charge transfer in CuNi alloys, one obtains good agreement between experimental and theoretical results for the bulk electronic density of states [24]. Thus, the Fermi energy E_f of the cleaved alloy is determined by using [12]

$$\int_{-\infty}^{E_f}\{C_A\cdot\varrho_{bA}(E)+C_B\cdot\varrho_{bB}(E)\}\,dE = C_A\cdot N_{Ni(Pd)}+C_B\cdot N_{Cu(Ag)}\,, \quad (18)$$

where $N_{Ni(Pd)}=9.4$ and $N_{Cu(Ag)}=10$ electrons.

One notices in Figs. 2 and 3 that mainly $\varrho_{Li}(E)$ of the first two layers is affected strongly by the surface; due to the surface $\varrho_{Ii}(E)$ and $\varrho_{IIi}(E)$ tend to narrow. Here it is interesting to note that this behavior on the $\varrho_{Li}(E)$ is common to the tight-binding models for the cleaved alloys (see Ref. [12]) and is independent of the inclusion of the off-diagonal disorders. On the other hand, one can see in Fig. 3 that the off-diagonal disorders influence significantly the electronic structures (total d-bandwidth) both for the surface and for the bulk layers.

4. Electronic Density of States for Chemisorbed Atoms on the Alloy Surface

Using the tight-binding theory for the cleaved alloys in Sect. 2, we calculate the local density of states for the single chemisorbed atom on alloy surfaces. In order to investigate the local atomic environment effects on the chemisorption behavior, we consider the six different adatom configurations; A (on-site), B (bridge-site), C (centered fourfold-site), C_{2A2B} (centered site coupled to two A-type and two B-type substrate atoms: $C2$ configuration in Ref. [12]), C_{4A} (centered site coupled to four A-type atoms), and C_{4B} (centered site coupled to four B-type atoms) configurations.

We calculate the local density of states for the chemisorbed atom, $\varrho_C(E)$, by the formula

$$\varrho_C(E)=-(1/\pi)\,\mathrm{Im}\,(E-E_C-\Delta_C)^{-1}\,, \quad (19)$$

where the self-energy for the chemisorbed atom Δ_C is given by

$$\Delta_C=\sum_i\frac{T_{Ci}^2}{E-E_{Ii}-\Delta_{Ii}} + \sum_{\substack{i\neq C\\ j\neq i,C}}\frac{T_{Ci}\,T_{ij}\,T_{jC}}{(E-E_{Ii}-\Delta_{Ii})(E-E_{Ij}-\Delta_{Ij}^{Ii})}\,. \quad (20)$$

Here, T^3 terms are included in order to get more detailed information on the adsorbate density of states. For the on-site and bridge-site configurations, the self-energies Δ_C are given by

$$\Delta_C=\frac{C_A\,T_{CA}^2}{E-E_{IA}-\Delta_{IA}}+\frac{C_B\,T_{CB}^2}{E-E_{IB}-\Delta_{IB}}\,, \quad (21)$$

and

$$\begin{aligned}\Delta_C = 2\Bigg\{&\frac{C_A T_{CA}^2}{E - E_{IA} - \Delta_{IA}} + \frac{C_B T_{CB}^2}{E - E_{IB} - \Delta_{IB}}\Bigg\} \\ &+ 2\Bigg\{\frac{C_A^2 T_{CA}^2 T_{AA}}{(E - E_{IA} - \Delta_{IA})(E - E_{IA} - \Delta_{IA}^{IA})} \\ &+ \frac{C_B T_{CB}^2 T_{BB}}{(E - E_{IB} - \Delta_{IB})(E - E_{IB} - \Delta_{IB}^{IB})} \\ &+ \frac{C_A C_B T_{CB} T_{BA} T_{AC}}{(E - E_{IA} - \Delta_{IA})(E - E_{IB} - \Delta_{IB}^{IA})} \\ &+ \frac{C_A C_B T_{CA} T_{AB} T_{BC}}{(E - E_{IB} - \Delta_{IB})(E - E_{IA} - \Delta_{IA}^{IB})}\Bigg\},\end{aligned} \tag{22}$$

respectively. The similar expressions are obtained for the C, C_{2A2B}, C_{4A}, and C_{4B} configurations.

In Figs. 4 and 5, we present the adsorbate density of states for the parameters, $C_A = 0.6$ and 0.8, $\delta_L = 0.6$, and $T_{AA} = 1.2\,T_{BB}$ ($T_{AB} = (T_{AA} \cdot T_{BB})^{1/2}$). In both figures, the curves (a) and (d) show the adatom density of states (single orbital per adatom) for the chemisorption system with $E_C = E_f$ and $T_{AC} = 3\,T_{AA}$: These parameter values roughly represent the gas atom adsorption on the alloy (CuNi, AuNi, etc.) surfaces. One notices in these figures that the effects of the chemisorption geometry on the behaviors of the $\varrho_C(E)$ are very

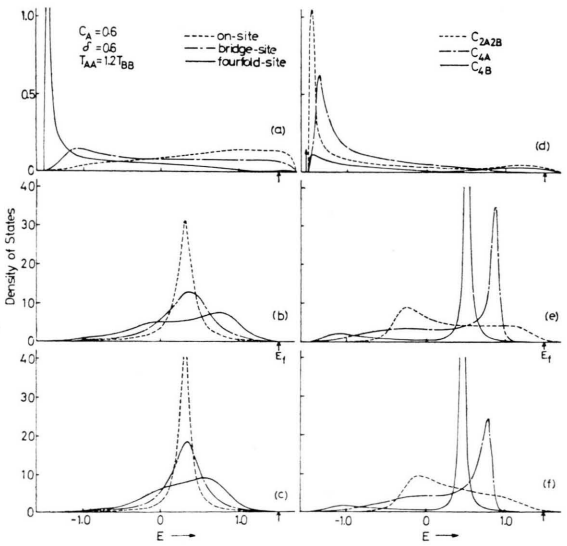

Fig. 4. Local density of states $\varrho_C(E)$ of the adatom on (100) cleaved fcc (CuNi) alloys for the A, B, C, C_{2A2B}, C_{4A}, and C_{4B} configurations. $C_A = 0.6$, $\delta = 0.6$, $T_{AA} = 1.2\,T_{BB}$. (a), (d) $E_C = E_f$ and $T_{AC} = 3\,T_{AA}$; (b), (e) $E_C = E_{A(Ni)}$ and $T_{AC} = 1.4\,T_{AA}$; (c), (f) $E_C = E_A$ and $T_{AC} = T_{AA}$.

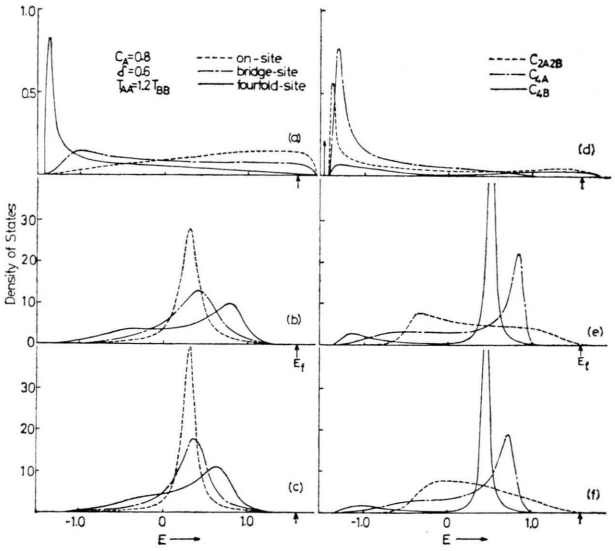

Fig. 5. Local density of states $\varrho_C(E)$ of the adatom on (100) cleaved (CuNi) alloys. $C_A = 0.8$. The other parameters and notations are the same as in Figure 4.

large. For example, one can observe the prominent peak (bonding resonance) near the lower band edge for the C, C_{2A2B}, C_{4A}, and C_{4B} configurations, in contrast to the A (on-site) and B (bridge-site) configurations.

The curves (b) and (e) in Figs. 4 and 5 show the adatom density of states for the system with $E_C = E_A$ and $T_{AC} = 1.4\,T_{AA}$, while the curves (c) and (f) are the results for the parameters $E_C = E_A$ and $T_{AC} = T_{AA}$. The parameters for the curves (b) and (e) roughly represent the Pd or Pt atom chemisorption on the (100) surface of the CuNi alloys and those for the (c) and (f) curves represent roughly the Ni atom chemisorption on the CuNi alloy surface. Again, the curves (b), (e), (c) and (f) demonstrate the importance of the local atomic environment effects on the chemisorption behavior; the adatom density of states strongly depends on the local atomic environment of the substrate atoms.

It is the most interesting that the resonance peaks (Lorentzian) for the C_{2A2B} configuration in Figs. 4 and 5 are located below the adsorbate energy level E_C ($= E_A > 0$). This behavior for the C_{2A2B} configuration is completely different from others and can not be understood from the general ideas for the adsorbate atom on the pure metal substrate (weak coupling picture of chemisorption) [26]. Following the general ideas of Ref. [26], the adsorbate resonance peak should be located above

E_C (if $E_C > 0$), as in the case of the other configurations. This surprising behavior of the resonance peak for the C_{2A2B} configuration results from the effects of the off-diagonal disorders in the substrate alloys and the hybridization of the energy levels of the adsorbate and substrate atoms E_A, E_B, and E_C. Therefore, in order to understand the chemisorption behavior on the alloy surface quantitatively, one has to take into account the effects of the off-diagonal disorders.

5. Atomic Segregation at the Surface of Binary Alloys

It is the aim of this section to study the surface segregation observed in the alloys like CuNi, AuNi, AgPd, and AgPt alloys [2—8], within the framework of the present theory. In view of the fact that, for instance, the d-bandwidth of Pd is about 80% wider than that of Ag [25], the effects of the off-diagonal disorder should be included in the theory. In order to investigate whether the atomic segregation occurs or not at the surface, we calculate the heat of segregation ΔQ_s. For the dilute binary alloys [15] the surface concentration of the solute, C_s, is related to its bulk concentration, C_b, by

$$C_s/(1 - C_s) = [C_b/(1 - C_b)] \exp(\Delta Q_s/kT). \quad (23)$$

If ΔQ_s is large and positive, then the surface segregation should occur. Even in the case of the concentrated alloys, the calculation of ΔQ_s is useful since it permits us to predict the segregation. Furthermore, the present calculation of ΔQ_s is much simpler than the calculation of the layer dependent concentrations C_i, based on the Lagrangian multiplier technique [13].

In order to calculate the heat of segregation ΔQ_s, we first investigate the changes in the electronic density of states due to the introduction of the additional B- (or A-) type atom in the surface (or subsurface) layer. The additional atom is regarded as an "impurity atom" in the effective medium of the disordered binary alloys. We assume here that only the local density of states of the atoms within the nearest-neighbour sites of the "impurity atom" are affected by the "impurity atom". The local density of states for the nearest-neighbour atoms (in the surface layer) of the B-type impurity atom is obtained as

$$\varrho_{IA}^{NN}(E) = -(1/\pi)\,\mathrm{Im}\,[E - E_{IA} - \Delta_{IA}^{NN}]^{-1}, \quad (24)$$

where

$$\Delta_{IA}^{NN} = \frac{(Z_0 - 1)\,C_A\,T_{AA}^2}{E - E_{IA} - \Delta_{IA}^{IA}} + \frac{\{(Z_0 - 1)\,C_B + 1\}\,T_{AB}^2}{E - E_{IB} - \Delta_{IB}^{IA}} + \frac{Z_1\,C_A\,T_{AA}^2}{E - E_{IIA} - \Delta_{IIA}^{IA}} + \frac{Z_1\,C_B\,T_{BB}^2}{E - E_{IIB} - \Delta_{IIB}^{IA}}, \quad (25)$$

$$\varrho_{IB}^{NN}(E) = -(1/\pi) \cdot \mathrm{Im}\,[E - E_{IB} - \Delta_{IB}^{NN}]^{-1}, \quad (26)$$

where

$$\Delta_{IB}^{NN} = \frac{(Z_0 - 1)\,C_A\,T_{AB}^2}{E - E_{IA} - \Delta_{IA}^{IB}} + \frac{\{(Z_0 - 1)\,C_B + 1\}\,T_{BB}^2}{E - E_{IB} - \Delta_{IB}^{IB}} + \frac{Z_1\,C_A\,T_{AB}^2}{E - E_{IIA} - \Delta_{IIA}^{IB}} + \frac{Z_1\,C_B\,T_{BB}^2}{E - E_{IIB} - \Delta_{IIB}^{IB}}. \quad (27)$$

The average electronic density of states for the nearest-neighbour atoms of the "impurity atom" is thus calculated by

$$\varrho_I^{NN}(E) = C_A \cdot \varrho_{IA}^{NN}(E) + C_B \cdot \varrho_{IB}^{NN}(E). \quad (28)$$

In the above equations (24)—(28), the pairs (NN, I), (NN, IA), and (NN, IB) indicate the nearest-neighbour atoms in the surface layer.

For the nearest-neighbour atoms (of the "impurity atom") in the second layer,

$$\varrho_{IIA(B)}^{NN}(E) = -(1/\pi) \cdot \mathrm{Im}\,[E - E_{IIA(B)} - \Delta_{IIA(B)}]^{-1}, \quad (29)$$

where

$$\Delta_{IIA} = \frac{(Z_1 - 1)\,C_A\,T_{AA}^2}{E - E_{IA} - \Delta_{IA}^{IIA}} + \frac{\{(Z_1 - 1)\,C_B + 1\}\,T_{AB}^2}{E - E_{IB} - \Delta_{IB}^{IIA}} + \frac{Z_0\,C_A\,T_{AA}^2}{E - E_{IIA} - \Delta_{IIA}^{IIA}} + \frac{Z_0\,C_B\,T_{AB}^2}{E - E_{IIB} - \Delta_{IIB}^{IIA}}, \quad (30)$$

$$\Delta_{IIB} = \frac{(Z_1 - 1)\,C_A\,T_{AB}^2}{E - E_{IA} - \Delta_{IA}^{IIB}} + \frac{\{(Z_1 - 1)\,C_B + 1\}\,T_{BB}^2}{E - E_{IB} - \Delta_{IB}^{IIB}} + \frac{Z_0\,C_A\,T_{AB}^2}{E - E_{IIA} - \Delta_{IIA}^{IIB}} + \frac{Z_0\,C_B\,T_{BB}^2}{E - E_{IIB} - \Delta_{IIB}^{IIB}}. \quad (31)$$

Therefore, the total changes in the electronic density of states due to the introduction of the B-type "impurity atom" in the surface layer is given by

$$\Delta_{Q_s}(E; B) = (1 - C_B)\,\varrho_{IB}(E) - C_A\,\varrho_{IA}(E) + Z_0[\varrho_I^{NN}(E) - \varrho_I(E)] + Z_1[\varrho_{II}^{NN}(E) - \varrho_{II}(E)], \quad (32)$$

where

$$\varrho_{II}^{NN}(E) = C_A\,\varrho_{IIA}^{NN}(E) + C_B\,\varrho_{IIB}^{NN}(E). \quad (33)$$

The change in the electronic energy $\Delta E_s(B)$ due to the introduction of the B-type "impurity atom" is thus obtained by the formula:

$$\Delta E_s(B) = \int_{-\infty}^{E_f} (E - E_f)\, \Delta\varrho_s(E; B)\, \mathrm{d}E\,. \qquad (34)$$

The heat of segregation of the B-type atom $\Delta Q_s(B)$ is defined as

$$\Delta Q_s(B) = \Delta E_{\mathrm{bulk}}(B) - \Delta E_s(B)\,, \qquad (35)$$

where $\Delta E_{\mathrm{bulk}}(B)$ is the change in the total electronic energy due to the introduction of the B-type "impurity atom" in the bulk layer.

In Fig. 6 we show the heat of segregation for the B (noble metal)-type atom ($E_B = -\delta/2$), ΔQ_s, as a function of concentration C_A for $\delta = 0.3$, 0.6 and $T_{AA} = T_{BB}$, $1.2\,T_{BB}$ ($T_{AB} = (T_{AA}\,T_{BB})^{1/2}$). These parameter values roughly represent the CuNi (or AuNi) alloys. The results in Fig. 6 show that the surface layer should be enriched in B (noble metal)-type atom for A(Ni) rich concentrations, in agreement with the experimental results as well as the previous theoretical results based on the elaborate Lagrangian multiplier technique [13]. The order of magnitude of ΔQ_s in Fig. 6 is comparable to that obtained by experiments for the AuNi (111) system [7], $\sim 12 \pm 2$ kcal/mole. Furthermore, one can see in Fig. 6 that the results of ΔQ_s are considerably affected by the inclusion of the off-diagonal disorders, even for the alloys such as CuNi alloys where the d-bandwidth of pure Ni is only about 20% wider then that of pure Cu. Thus, for the quantitative understanding of the surface phenomena of the disordered alloys like AgPd, RhNi, PtNi, and AuNi, the effects of the off-diagonal disorders have to be included.

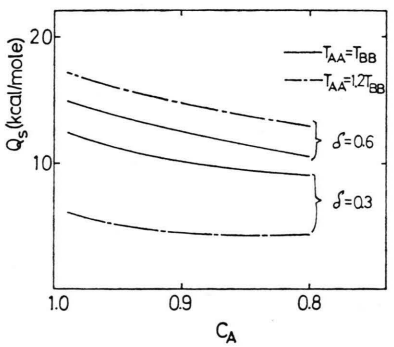

Fig. 6. Heat of segregation ΔQ_s (kcal/mole) for the B(noble metal)-type atom as a function of the concentration $C_{A(Ni)}$.

Finally, we note that the present formulation for obtaining the heat of surface segregation can be straightforwardly used to study the segregation of solute to the stacking faults or grain boundaries [27].

6. Concluding Remarks

We have investigated the electronic structure of alloy surfaces including both diagonal and off-diagonal disorder in the tight-binding Hamiltonian and demonstrated that the off-diagonal disorder can influence significantly the electronic structure. The present method has the advantage that it is capable of treating the general off-diagonal disorder without difficult and extensive numerical calculations. The electronic density of states of cleaved alloys as well as of the bulk alloys are calculated using the first terms in the continued fraction series for the Green's function. The overall shape of the density of states is essentially the same as that obtained by using the much more elaborate method of Ref. [14, 23]. The iterative procedure for obtaining the electronic Green's function is found to work quite well even when off-diagonal disorder is included: After 20 or 30 iterations, the self-energies of the type Δ_j^i converge to the final values.

In addition, we have studied the chemisorption and segregation behavior of cleaved alloys in detail. The parameters are chosen to describe transition metal alloys like CuNi, AuNi, or AgPd alloys. In the calculation of the adsorbate electronic density of states (Ni, Pd, and Pt atom chemisorption on the CuNi (100) surface), we have found a new resonance peak for the C_{2A2B} configuration, where the energy of the resonance peak is not directly related to the orbital energy of the adsorpate atom, in contrast to the single atom chemisorption (weak coupling) on the pure metal substrate. The resonance energy is determined, in a rather complicated way, by the hopping integrals (T_{AA}, T_{AB}, T_{BB}, T_{AC}, and T_{BC}) and the atomic energies (E_A, E_B, and E_C) of the substrate and adsorbate atoms. Thus, the off-diagonal disorder in the tight-binding alloy Hamiltonian does play an important role in chemisorption on alloy surfaces.

The surface segregation behavior of alloys like CuNi (or AuNi) alloys has been studied by calculating the heat of segregation ΔQ_s, instead of undertaking the elaborate calculation based on the

Lagrangian multiplier technique [13]. The formulation for obtaining the heat of surface segregation, ΔQ_s, is presented not only because it is numerically simple but also because it can be straightforwardly used to study the segregation of solute at the stacking faults or grain boundaries, which are very important for the understanding of the mechanical properties of the materials. To our knowledge, this is the first time that a microscopic electronic theory has been used to calculate the heat of segregation ΔQ_s. The numerical results of ΔQ_s for the CuNi (or AuNi) alloys indicate that the noble (Cu or Au) metal atoms tend to segregate in the surface layer, in agreement with experiments. We have also found that the ΔQ_s are strongly influenced by the inclusion of the off-diagonal disorder even when the difference between the bandwidths of pure A and B metals is approximately 20% of the pure metal bandwidth. Thus, it is concluded that in order to understand the segregation behavior of cleaved alloys quantitatively, the effect of the off-diagonal disorder has to be included.

The present theory for cleaved alloys can further be used to study the electronic structure of semi-infinite crystals with two dimensional substitutional disorder in the outermost layer as well as to investigate the changes in the electronic density of states due to the order-disorder phase transition in chemisorbed layers. Such applications are presented in Appendices A and B, respectively.

Acknowledgement

The author would like to thank Professor T. Mori for valuable discussions. He is also grateful to the Sakkokai Foundation for the financial support.

Appendix A

Here, we apply the present tight-binding theory for cleaved alloys to study the electronic structures of the metal surface with substitutional disorder. Recently, several authors [18—20] have extended the Kalkstein-Soven [17] theory for semi-infinite crystals in such a way that the random distribution of impurity atoms in the surface layer (two dimensional disorder alloy) can be discussed. These extensions are of great importance for the studies of the surface segregation of dilute alloys [15—16], the diffusion behavior of surface impurities into a bulk [27], and other related surface phenomena. However, the previous Green's function theories are probably incapable of treating the off-diagonal disorders introduced in the outermost layer, since it is difficult to estimate the effective transfer integrals between the atomic sites in the first layer and those in the second layer.

Now, we investigate, within the framework of the present theory, the electronic structure of the metal surface with substitutional disorder including both the diagonal and off-diagonal disorders. The formalism is quite parallel to that for the cleaved alloys in Section 2. In Eqs. (6)—(9), we simply take such that $E_{\mathrm{IIA}}=E_{\mathrm{IIB}}$, $E_{\mathrm{IIIA}}=E_{\mathrm{IIIB}}$, and $E_{b\mathrm{A}}=E_{b\mathrm{B}}$ (in the following, B refers to the surface impurities), and obtain the following expressions for the self-energies:

$$\Delta_{\mathrm{IA}}=\frac{Z_0\,C_{\mathrm{A}}\,T_{\mathrm{AA}}^2}{E-E_{\mathrm{IA}}-\Delta_{\mathrm{IA}}^{\mathrm{I}}}+\frac{Z_0\,C_{\mathrm{B}}\,T_{\mathrm{AB}}^2}{E-E_{\mathrm{IB}}-\Delta_{\mathrm{IB}}^{\mathrm{I}}}+\frac{Z_1\,T_{\mathrm{AA}}^2}{E-E_{\mathrm{IIA}}-\Delta_{\mathrm{II}}^{\mathrm{I}}}, \tag{A.1}$$

$$\Delta_{\mathrm{IB}}=\frac{Z_0\,C_{\mathrm{A}}\,T_{\mathrm{BA}}^2}{E-E_{\mathrm{IA}}-\Delta_{\mathrm{IA}}^{\mathrm{I}}}+\frac{Z_0\,C_{\mathrm{B}}\,T_{\mathrm{BB}}^2}{E-E_{\mathrm{IB}}-\Delta_{\mathrm{IB}}^{\mathrm{I}}}+\frac{Z_1\,T_{\mathrm{BA}}^2}{E-E_{\mathrm{IIA}}-\Delta_{\mathrm{II}}^{\mathrm{I}}}, \tag{A.2}$$

$$\Delta_{\mathrm{II}}=\frac{Z_0\,T_{\mathrm{AA}}^2}{E-E_{\mathrm{IIA}}-\Delta_{\mathrm{II}}^{\mathrm{II}}}+\frac{Z_1\,T_{\mathrm{AA}}^2}{E-E_{\mathrm{IIIA}}-\Delta_{\mathrm{III}}^{\mathrm{II}}}+\frac{Z_1\,C_{\mathrm{A}}\,T_{\mathrm{AA}}^2}{E-E_{\mathrm{IA}}-\Delta_{\mathrm{IA}}^{\mathrm{II}}}+\frac{Z_1\,C_{\mathrm{B}}\,T_{\mathrm{AB}}^2}{E-E_{\mathrm{IB}}-\Delta_{\mathrm{IB}}^{\mathrm{II}}}, \tag{A.3}$$

$$\Delta_{\mathrm{III}}=\frac{Z_0\,T_{\mathrm{AA}}^2}{E-E_{\mathrm{IIIA}}-\Delta_{\mathrm{III}}^{\mathrm{III}}}+\frac{Z_1\,T_{\mathrm{AA}}^2}{E-E_{\mathrm{IIA}}-\Delta_{\mathrm{IIA}}^{\mathrm{III}}}+\frac{Z_1\,T_{\mathrm{AA}}^2}{E-E_{b\mathrm{A}}-\Delta_{b\mathrm{A}}^{\mathrm{III}}}. \tag{A.4}$$

The expressions for the self-energies of the types, $\Delta_{\mathrm{IA}}^{\mathrm{I}}$, $\Delta_{\mathrm{IB}}^{\mathrm{I}}$, $\Delta_{\mathrm{II}}^{\mathrm{I}}$, ..., are obtained by using Equation (3b). Again, we solve the coupled equations for the self-energies by iteration.

Numerical calculations of $\varrho_L(E)$ for $L=1$ are carried out for the (100) surface of the simple cubic metal with a complete disorder in the surface layer. In Fig. 7, we show the average electronic density of states of the outermost layer, $\varrho_{\mathrm{I}}(E)$ for the parameters: $C_{\mathrm{A}}=0.2$, 0.5 and 0.9, $T_{\mathrm{AB}}=(T_{\mathrm{AA}}\cdot T_{\mathrm{BB}})^{1/2}$; (a) $T_{\mathrm{BB}}=T_{\mathrm{AA}}/2$, $E_{\mathrm{IA}}(=E_{\mathrm{IIA}}=E_{\mathrm{IIIA}}=E_{b\mathrm{A}})=0$, $E_{\mathrm{IB}}=0.5$ (in units of the half-bandwidth of the pure A metal), (b) $T_{\mathrm{BB}}=1.5\,T_{\mathrm{AA}}$, $E_{\mathrm{IA}}=E_{\mathrm{IB}}=0$.

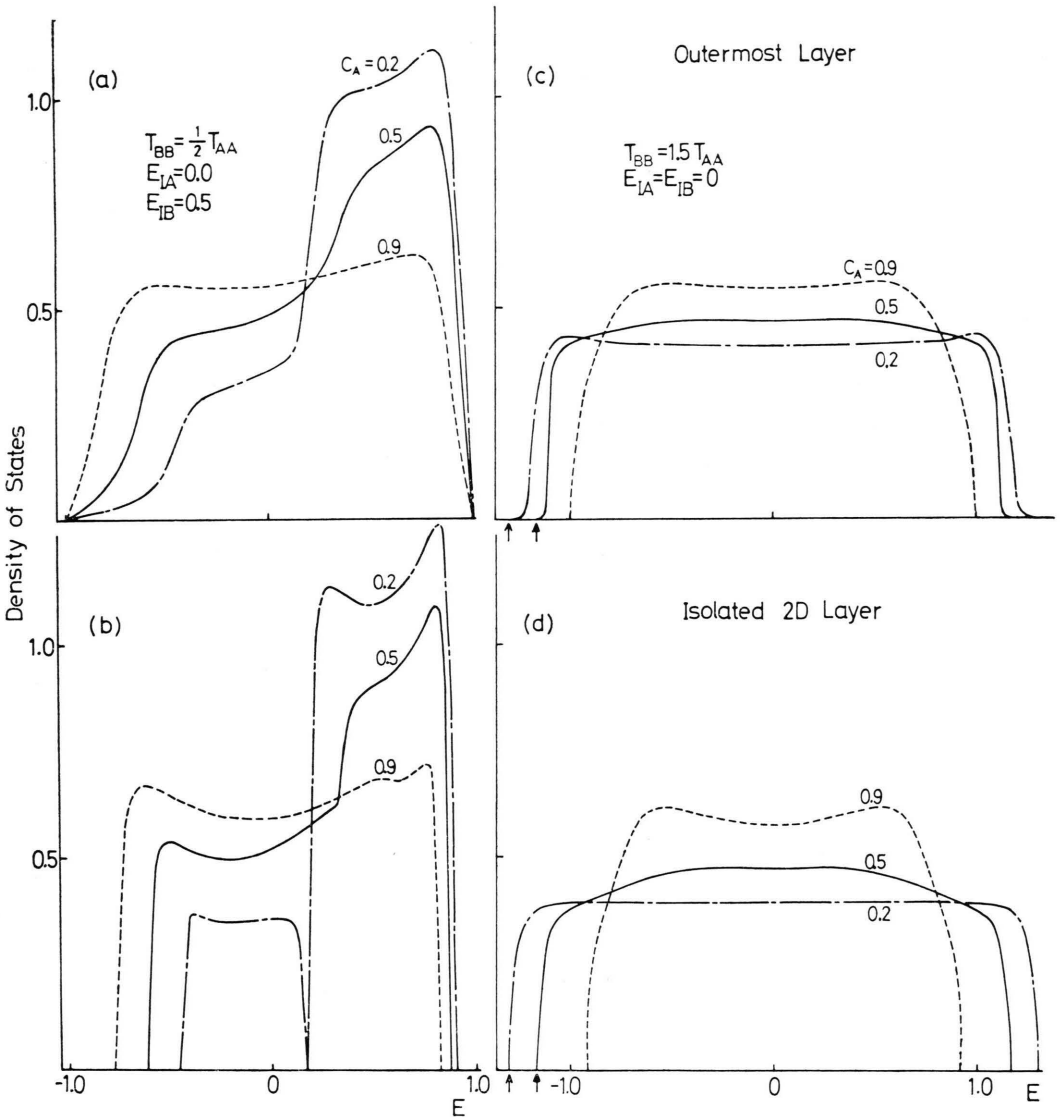

Fig. 7. Comparison of the electronic density of states of the sc metal surface with substitutional disorder [(a), (c)] with that of the uncoupled two-dimensional random alloy [(b), (d)]. $C_A = 0.2$, 0.5 and 0.9. (a), (b) $T_{BB} = T_{AA}/2$, $E_{IA} = 0$, and $E_{IB} = 0.5$; (c), (d) $T_{BB} = 1.5\, T_{AA}$ and $E_{IA} = E_{IB} = 0$. The energy is in units of the half-bandwidth of the pure A-type metal. The electronic density of states of the clean surface ($C_A = 1$, $E_{IA} = E_{IIA} = E_{IIIA} = E_{bA}$) is the same as in Appendix B and presented in Fig. 8 (dashed curve).

For comparison, we have also presented the electronic density of states for the corresponding two-dimensional random alloys. One can see that the coupling effect to the semi-infinite metals on the electronic structures is considerably strong.

Appendix B

In this Appendix, we investigate the changes in the electronic density of states due to the order-disorder phase transition in chemisorbed layers. In particular, we give the formulation appropriate for the chemsiorption systems such as the (alkali adsorbate)/(noble or transition metal substrate) systems, where the direct interaction between the adatoms plays an important role and the tight-binding approximation may be used [29]. For the illustrative purpose, we consider the chemisorption system with $\Theta = 1/2$, where Θ is the adsorbate coverage and assume that A-type chemisorbed

atoms are in the on-site position of the (100) surface of a B-type sc metal. For comparison, we consider two types of the ordered structures, $C(2\times 2)$ and (2×1) structures.

We now divide the whole chemisorbed system into two sublattices α and β, such that there are $N/2$ sites of type α and $N/2$ sites of type β. The atomic order parameter η for the chemisorbed layer is defined as follows:

$$P_\alpha^{\mathrm{A}} = P_\beta^{\mathrm{V}} = (1+\eta)/2,$$
$$P_\alpha^{\mathrm{V}} = P_\beta^{\mathrm{A}} = (1-\eta)/2, \tag{B.1}$$

where $P_\alpha^{\mathrm{A}}(P_\alpha^{\mathrm{V}})$ and $P_\beta^{\mathrm{A}}(P_\beta^{\mathrm{V}})$ are the probabilities to find an A-atom (a vacancy) in the α and β sublattice, respectively. If $\eta=1$ (the complete order case) all chemisorbed atoms are on the α sublattice and the β sublattice is empty (occupied by vacancies). If $\eta=0$ (the complete disorder case) there are as many as chemisorbed atoms on α sites and β sites and the same holds for vacancies. By considering the atomic rows perpendicular to the surface plane, the substrate atoms are divided into α and β sublattices as well: If the outermost chemisorbed atom is sitting in the $\alpha(\beta)$ lattice, the substrate atoms beneath it are on the $\alpha(\beta)$ lattice.

For the case of $C(2\times 2)$ adsorbate structure, where each $\alpha(\beta)$-site has Z_0 $\beta(\alpha)$-sites within the same layer and Z_1 $\alpha(\beta)$-sites within the adjacent layer as its nearest-neighbours, the self-energies for the adsorbate layer are expressed as

$$\Delta_{\mathrm{A}\alpha}(\eta) = \frac{Z_0\, P_\beta^{\mathrm{A}}\, T_{\mathrm{AA}}^2}{E - E_{\mathrm{A}\beta} - \Delta_{\mathrm{A}\beta}^{\mathrm{A}\alpha}(\eta)} + \frac{Z_1\, T_{\mathrm{AB}}^2}{E - E_{\mathrm{I}\alpha} - \Delta_{\mathrm{I}\alpha}^{\mathrm{A}\alpha}(\eta)}, \tag{B.2}$$

$$\Delta_{\mathrm{A}\beta}(\eta) = \frac{Z_0\, P_\alpha^{\mathrm{A}}\, T_{\mathrm{AA}}^2}{E - E_{\mathrm{A}\alpha} - \Delta_{\mathrm{A}\alpha}^{\mathrm{A}\beta}(\eta)} + \frac{Z_1\, T_{\mathrm{AB}}^2}{E - E_{\mathrm{I}\beta} - \Delta_{\mathrm{I}\beta}^{\mathrm{A}\beta}(\eta)}. \tag{B.3}$$

The corresponding self-energies for the (2×1) adsorbate structure, where each $\alpha(\beta)$-site has $Z_0/2$ α-sites and $Z_0/2$ β-sites within the same layer and Z_1 $\alpha(\beta)$-sites within the adjacent layer as its nearest-neighbours, are given by

$$\Delta_{\mathrm{A}\alpha}(\eta) = \frac{(Z_0/2)\, P_\alpha^{\mathrm{A}}\, T_{\mathrm{AA}}^2}{E - E_{\mathrm{A}\alpha} - \Delta_{\mathrm{A}\alpha}^{\mathrm{A}\alpha}(\eta)} + \frac{(Z_0/2)\, P_\beta^{\mathrm{A}}\, T_{\mathrm{AA}}^2}{E - E_{\mathrm{A}\beta} - \Delta_{\mathrm{A}\beta}^{\mathrm{A}\alpha}(\eta)} + \frac{Z_1\, T_{\mathrm{AB}}^2}{E - E_{\mathrm{I}\alpha} - \Delta_{\mathrm{I}\alpha}^{\mathrm{A}\alpha}(\eta)}, \tag{B.4}$$

$$\Delta_{\mathrm{A}\beta}(\eta) = \frac{(Z_0/2)\, P_\alpha^{\mathrm{A}}\, T_{\mathrm{AA}}^2}{E - E_{\mathrm{A}\alpha} - \Delta_{\mathrm{A}\alpha}^{\mathrm{A}\beta}(\eta)} + \frac{(Z_0/2)\, P_\beta^{\mathrm{A}}\, T_{\mathrm{AA}}^2}{E - E_{\mathrm{A}\beta} - \Delta_{\mathrm{A}\beta}^{\mathrm{A}\beta}(\eta)} + \frac{Z_1\, T_{\mathrm{AB}}^2}{E - E_{\mathrm{I}\beta} - \Delta_{\mathrm{I}\beta}^{\mathrm{A}\beta}(\eta)}. \tag{B.5}$$

The self-energies for the substrate layers and those for the types of $\Delta_{\mathrm{A}\beta}^{\mathrm{A}\alpha}(\eta)$, $\Delta_{\mathrm{I}\alpha}^{\mathrm{A}\alpha}(\eta)$, ..., are obtained from Equation (3b). Here, it is noted that the approximation on Δ_i^{ij} should become better at the adsorbate layer, since the number of neglected paths of the electron hopping processes is smaller than that for the surface layer.

In Fig. 8 we show the electronic density of states of the adatom $\varrho_{\mathrm{A}}(E)$ for the $C(2\times 2)$ and (2×1) adlayers as a function of the order parameter η, with parameters $E_{\mathrm{A}\alpha}=E_{\mathrm{A}\beta}=0.1$ and $E_{\mathrm{I}\alpha}=E_{\mathrm{I}\beta}=0$. The energy E is given in units of the half-bandwidth

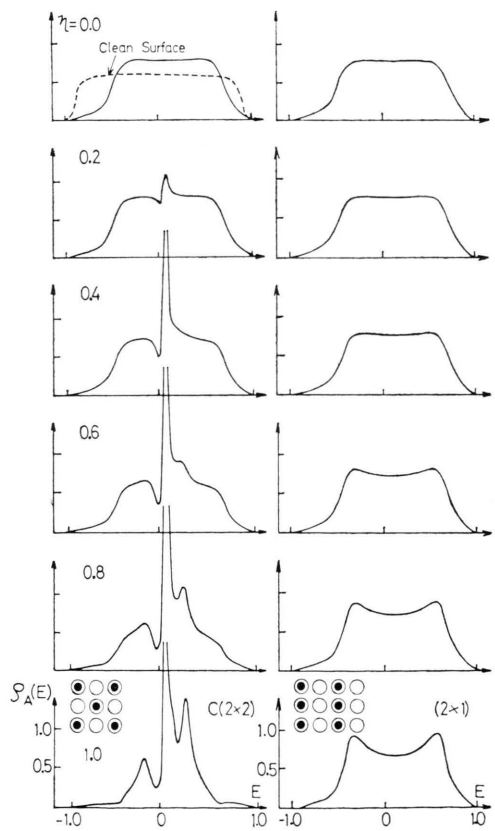

Fig. 8. Local density of states of the adatom $\varrho_{\mathrm{A}}(E)$ as a function of the order parameter η for the $C(2\times 2)$ and (2×1) adlayers. $E_{\mathrm{A}\alpha}=E_{\mathrm{A}\beta}=0.1$, $E_{\mathrm{I}\alpha}=E_{\mathrm{I}\beta}=0$, and $T_{\mathrm{AA}}=T_{\mathrm{BB}}=T_{\mathrm{AB}}$ (B refers to the substrate atom). The energy is in units of the half-bandwidth of the substrate (B-type) metal.

of the substrate metal. One can see in Fig. 8 that $\varrho_A(E)$ strongly depends on the local atomic environment of the adatom. For the $C(2 \times 2)$ adlayer, as η increases the adatom band becomes narrower and has the more detailed structure while for the (2×1) adlayer there are not so drastic changes in $\varrho_A(E)$.

[1] J. H. Sinfelt, J. L. Carter, and D. J. C. Yates, J. Catalysis **24**, 283 (1972).
[2] J. H. Sinfelt, J. Catalysis **29**, 308 (1973).
[3] R. Bouwman and W. Sachtler, J. Catalysis **19**, 127 (1970).
[4] K. Christman and G. Ertl, Surf. Sci. **33**, 254 (1972).
[5] F. L. Williams and M. Boudart, J. Catalysis **30**, 438 (1973).
[6] C. R. Helms, J. Catalysis **36**, 114 (1975).
[7] J. J. Burton, C. R. Helms, and R. S. Polizzotti, J. Vac. Sci. Tech. **13**, 204 (1976); J. Chem. Phys. **65**, 1089 (1976).
[8] P. Heimann, H. Neddermeyer, and M. Pessa, Phys. Rev. B **17**, 427 (1978).
[9] R. S. Polizzotti and J. J. Burton, J. Vac. Sci. Tech. **14**, 347 (1977).
[10] N. F. Berk, Surf. Sci. **48**, 289 (1975).
[11] J. L. Morán-López, G. Kerker, and K. H. Bennemann, J. Phys. F **5**, 1277 (1975).
[12] J. L. Morán-López, G. Kerker, and K. H. Bennemann, Surf. Sci. **57**, 540 (1976).
[13] G. Kerker, J. L. Morán-López, and K. H. Bennemann, Phys. Rev. B **15**, 638 (1977).
[14] M. C. Desjonquères and F. Cyrot-Lackmann, J. Phys. F **7**, 61 (1977).
[15] J. J. Burton and R. S. Polizzotti, Surf. Sci. **66**, 1 (1977).
[16] H. P. Stuwe and I. Jager, Acta Met. **24**, 605 (1976).
[17] D. Kalkstein and P. Soven, Surf. Sci. **26**, 85 (1971).
[18] I. Ishida, N. Inoue, and T. Matsubara, Prog. Theor. Phys. **55**, 653 (1976).
[19] B. Velický and J. Kudrnovský, Surf. Sci. **64**, 411 (1977).
[20] K. Masuda, Prog. Theor. Phys. **58**, 696 (1977); Phys. Lett. **64** A, 65 (1977).
[21] J. L. Jacobs, J. Phys. F **3**, 933 (1973).
[22] H. Shiba, Prog. Theor. Phys. **46**, 77 (1971).
[23] J. A. Blackman, D. M. Esterling, and N. F. Berk, Phys. Rev. B **4**, 2412 (1971).
[24] C. M. Stocks, R. W. Williams, and J. S. Faulkner, Phys. Rev. B **4**, 4390 (1971).
[25] H. Ehrenreich and L. M. Schwartz, Solid State Phys. Academic Press **31**, 149 (1976).
[26] T. L. Einstein, Phys. Rev. B **12**, 1262 (1975). W. Ho, S. L. Cunningham, and W. H. Weinberg, Surf. Sci. **54**, 139 (1976). K. Masuda, Z. Naturforsch. **31a**, 1344 (1976).
[27] P. R. Howell, D. E. Fleet, A. Hildon, and B. Ralph, J. Microsc. **107**, 155 (1976).
[28] M. Leynaud and G. Allan, Surf. Sci. **53**, 359 (1975).
[29] S. Anderson, Electronic Structure and Reactivity of Metal Surfaces, ed. by E. G. Derouane and A. A. Lucas, Plenum, 1976, p. 289. A. G. Naumovets and A. G. Fedorus, JETP Letters **10**, 6 (1969). L. D. Schmidt, J. Vac. Sci. Techn. **9**, 882 (1972).
[30] J. L. Morán-López and A. ten Bosch, Surf. Sci. **68**, 377 (1977). K. Masuda, to be published.